Supporting Information

Hierarchical-porous metal-organic frameworks fabricated through solvent-assisted strategy with high catalytic activity

Peng Wang,‡[b] Peng Zhang,‡[a] Yu Shen,‡[a] Liu Wang,[a] Hongfeng Li,[a] Wenlei Zhang,[b] Zhida Gu,[b] Xinglong Zhang,[a] Yu Fu,*[b] Weina Zhang*[a] and Fengwei Huo*[a]

[a]Key Laboratory of Flexible Electronics (KLOFE) & Institute of Advanced Materials (IAM), Nanjing Tech University (NanjingTech), 30 South Puzhu Road, Nanjing 211816, China.

[b]College of Science, Northeastern University, Shenyang 100819, China.

‡These authors contributed equally.

Materials and Instrumentation

All chemicals were purchased from commercial sources and used without further purification. All solvents are purchased from Sinopharm. The brands of other chemicals are listed in the synthesis method. X-ray diffraction (XRD) patterns of samples were recorded with Smartlab X-ray diffractometer (3kW, Rigaku, Japan) using nickel-filtered Cu Kα radiation (λ = 1.5406 Å). Scanning electron microscope (SEM) images were taken by JEOL JSM-7800F. Transmission electron microscope (TEM) images were taken by JEOL JEM-2100Plus at an accelerating voltage of 200 kV. The JEOL JEM-2100F is also equipped with an energy dispersive X-ray spectrometer (EDX) system and allows the elemental analysis of samples. Thermo gravimetric analyses (TGA) were performed on Mettler-Toledo TGA2 under nitrogen gas flow at 5 °C min^{-1} from 100 °C to 800 °C. The pore textural properties including Brunauer-Emmett-Teller (BET) surface area, pore volume, and pore size were obtained by analyzing N_2 adsorption and desorption isotherms with Micromeritics ASAP 2460 built-in software. Before starting the adsorption measurements, each sample was activated by heating under vacuum at 523 K for 20 h. UV-vis spectra were recorded on a Shimadzu UV-1750 spectrophotometer. Gas chromatography (GC) spectra were recorded on Agilent Technologies 7890B (equipped with HP-5 column and flame ionization detector) and gas chromatography mass spectrometry (GC-MS) spectra were analyzed by Agilent Technologies 7890B/5977B. Inductively coupled plasma (ICP) spectroscopy was conducted on PerkinElmer Avio200.

Experimental Section

Synthesis of MOFs

UiO-66-COOH: 1.8 g 1,2,4-benzenotricarboxylic acid (Aladdin, 98%), 1.0 g zirconyl nitrate ($ZrO(NO_3)_2 \cdot H_2O$, Macklin, 99%) and 15.8 g benzoic acid was dissolved in 30 mL N,N-Dimethylformamide (DMF) solution at room temperature via ultrasonication.[1] The mixture was then sealed in a Teflon reactor (100 mL) and allowed to react at 150 ^oC for 24 h without stirring. After cooling to room temperature, then the white precipitate was collected by centrifugation and washing with 20 mL DMF and 20 mL ethanol for three times, respectively. Finally, the resulting white powder was dried at 120 °C for 24 h.

UiO-66: 23.3 mg zirconium chloride ($ZrCl_4$, 10 mM, Energy Chemical, 98%),16.8 mg 1,4-dicarboxybenzene (10 mM, Sigma, 98%) and 1.37 mL acetic acid were dissolved in 10 mL DMF in a 40 mL glass sample vial by ultrasonic for about 1 min, and then the vial was capped and placed into an oven preheated at 120 °C for 24 h.[2] The product was collected by centrifugation and washing with 20 mL DMF and 20 mL ethanol for three times, respectively. Finally, the resulting powder was dried at 120 °C for 24 h.

UiO-66-OH: 23.3 mg zirconium chloride ($ZrCl_4$, 10 mM), 18.2 mg 2-hydroxyterephthalic acid (10 mM, Sigma, 97%) and 1.37 mL acetic acid were dissolved in 10 mL DMF in a 40 mL glass sample vial by ultrasonic for about 1 min, and then the vial was capped and placed into an oven preheated at 120 °C for 24 h. The product was collected by centrifugation and washing with 20 mL DMF and 20 mL ethanol for three times, respectively. Finally, the resulting powder was dried at 120 °C for 24 h.

UiO-66-2OH: 23.3 mg zirconium chloride ($ZrCl_4$, 10 mM), 9.9 mg 2,5-dihydroxyterephthalic acid (5 mM, Sigma, 98%) and 1.37 mL acetic acid were dissolved in 10 mL DMF in a 40 mL glass sample vial by ultrasonic for about 1 min, and then the vial was capped and placed into an oven preheated at 120 °C for 24 h. The product was collected by centrifugation and washing with 20 mL DMF and 20 mL ethanol for three times, respectively. Finally, the resulting powder was dried at 120 °C for 24 h.

UiO-66-NH_2: 23.3 mg zirconium chloride ($ZrCl_4$, 10 mM), 18.1 mg 2-aminoterephthalic acid (10 mM, Sigma, 99%) and 1.37 mL acetic acid were dissolved in 10 mL DMF in a 40 mL glass sample vial by ultrasonic for about 1 min, and then the vial was capped and placed into an oven preheated at 120 °C for 24 h. The product was collected by centrifugation and washing with 20 mL DMF and 20 mL ethanol for three times, respectively. Finally, the resulting powder was dried at 120 °C for 24 h.

MIL-125: 1.67 g 1,4-dicarboxybenzene (0.3 M) was dissolved in 30 mL DMF and 3.33 mL methanol solution in 50 mL Teflon reactor by ultrasonic for about 5 min, then 0.87 mL titanium isopropoxide (Energy Chemcial, 99%) was added the Teflon reactor and stirring for 30 min.[3] The substrate mixture was transferred to oven and heated at 150 °C for 24 h. The product was collected by centrifugation and washing with 20 mL DMF and 20 mL ethanol for three times, respectively. Finally, the resulting powder was dried at 120 °C for 24 h.

MIL-88-NH_2: 15 mL DMF dispersion of $Fe(NO_3)_3 \cdot 9H_2O$ (0.33 M, Sigma, 98%) was added to a glass bottle with 15 mL DMF dispersion of 2-aminoterephthalic acid (0.33

M) and ultrasonic for about 1 min.[4] Then, it was then heated at 120 °C for 24 h. The product was collected by centrifugation and washing with 20 mL DMF and 20 mL ethanol for three times, respectively Finally, the resulting powder was dried at 120 °C for 24 h.

HKUST-1: 50 mL methanol dispersion of 1.82 g copper nitrate trihydrate ($Cu(NO_3)_2 \cdot 3H_2O$, 75 mM, Sigma, 99%) was added to a beaker with 50 mL methanol dispersion of 0.875 g 1,3,5-Benzenetricarboxylic acid (H_3BTC, 53 mM, Sigma, 95%) and ultrasonic for about 1 min.[5] Then, it kept room temperature for 2 h in a standing. The product was collected by centrifugation and washing with 20 mL DMF and 20 mL ethanol for three times, respectively. Finally, the resulting powder was dried at 120 °C for 24 h.

MIL-101(Cr): 0.40 g chromic nitrate nonahydrate ($Cr(NO_3)_3 \cdot 9H_2O$, 0.1 mM, Sigma, 99.99%), 0.11 g 1,4-dicarboxybenzene (0.066 mM) and deionized water (10 mL) were blended and briefly stirred, resulting in a dark blue suspension.[6] The suspension was placed in a Teflon lined autoclave and kept in an oven at 180 °C for 4 h without stirring. The product was collected by centrifugation and washing with 20 mL DMF and 20 mL ethanol for three times, respectively. Finally, the resulting powder was dried at 120 °C for 24 h.

Synthesis of non-porous CPs

CoBTC: 0.2 g Cobalt(II) acetate tetrahydrate ($C_4H_6CoO_4 \cdot 4H_2O$ 20 mM, Sigma, 98%) and 1.2 g PVP (Mw = 29,000, Sigma) was dissolved into the mixed solution of ethanol (20 mL) and deionized water (20 mL), formed solution A, which was put on the

magnetic stirrer with a low speed.[7] 0.36 g H_3BTC (43 mM) was dissolved into the mixed solution of ethanol (20 mL) and deionized water (20 mL), formed solution B. Then solution B was poured into solution A with a constant speed by using an injector (10 mL). The mixed solution was kept stirring until the precipitation formed. Then centrifuged the product after standing for 24 hours and washed with 20 mL DMF and 20 mL ethanol for three times, respectively. Finally, the resulting powder was dried at 80 °C for 12 h.

CuSIP: 5 mL 99.825 mg water dispersion of copper nitrate hydrate ($Cu(NO_3)_2 \cdot 3H_2O$) was added to a glass bottle with 5 mL 67.04 mg methanol dispersion of 5-sulfoisophthalic acid sodium salt (NaH_2SIP, Aladdin, 98%) and briefly stirred.[8] Then centrifuged the product after standing for 24 hours and washed with 20 mL DMF and 20 mL ethanol for three times, respectively. Finally, the resulting powder was dried at 120 °C for 24 h.

Synthesis HP-MOFs or HP-CPs

In a typical synthesis, the HP-MOFs or HP-CPs can be obtained as follows: 30 mg pristine MOFs or CPs was dispersed into 30 mL alcohol by stirring for 1 h. The mixture was then sealed in a Teflon reactor (50 mL) and allowed to react at different temperature for different time without stirring. Then the precipitate was collected by centrifugation and washing with 20 mL ethanol for three times. Finally, the resulting powder was dried in vacuum oven for 24 h. The detailed treated temperature, time and solvent are listed in Table S1.

Catalytic reaction

Before catalysis, each catalyst was dried at 150 °C under vacuum to remove residual solvent molecules.

Ring opening reaction of styrene oxide with methanol:

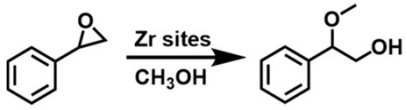

The catalyst (UiO-66-COOH or HP-UiO-66-COOH 15 mg) and styrene oxide (0.25 mmol, TCI, 98%) were put into a 5 mL glass bottle in methanol (2 mL).[9] Dodecane (20 μL, Energy Chemical, 98%) as internal standard. The reaction mixture was stirred for the 24 h in air at room temperature. After the reaction, the catalyst powder was filtered off and the filtrate was analyzed using a GC.

The reusability of HP-UiO-66-COOH composite was examined by monitoring its ring opening reaction of styrene oxide activities. At the end of the reaction, the heterogeneous mixture was centrifuged and washed with methanol for several times. The recovered catalyst was then activated at 150 °C for the subsequent recycling reaction.

Oxidation of diphenylmethane:

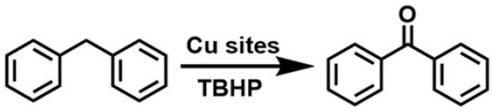

The oxidation of diphenylmethane reaction was carried out in 1 mL acetonitrile (Sigma, 99.9%). In a typical experiment, 5 mg catalysts (HKUST-1 or HP-HKUST-1) was loaded in a reactor.[10] 1 mL acetonitrile, tert-Butyl hydroperoxide (TBHP, 0.312 mmol, Energy Chemical, 70% solution in water) and dodecane (20 μL) as internal standard

were added in the reactor and the mixture was sonicated for 5 min to afford a homogeneous suspension. Diphenylmethane (0.125 mmol, Aladdin, 99%) was then added in the reactor and the mixture was sonicated again for 5 min, the reaction was allowed to proceed at 70 °C for 5 h. After the reaction, the catalyst powder was filtered off and the filtrate was analyzed using a gas chromatograph.

Oxidation of styrene:

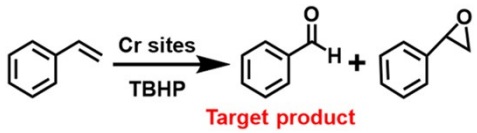

In a typical experimental, a 25 mL round bottomed flask was added 10 mg catalysts (MIL-101(Cr) or HP-MIL-101(Cr)), TBHP (6 mmol) and acetonitrile (10 mL) and the mixture was sonicated for 5 min.[6] After then styrene (2 mmol, Energy Chemical, 99.5%) was charged into the solution. The reaction is performed at 80 °C with stirring in oil bath and refluxed at 80 °C for 12 h. After the reaction, the catalyst powder was filtered off and the filtrate was analyzed using a gas chromatograph.

Characterization：

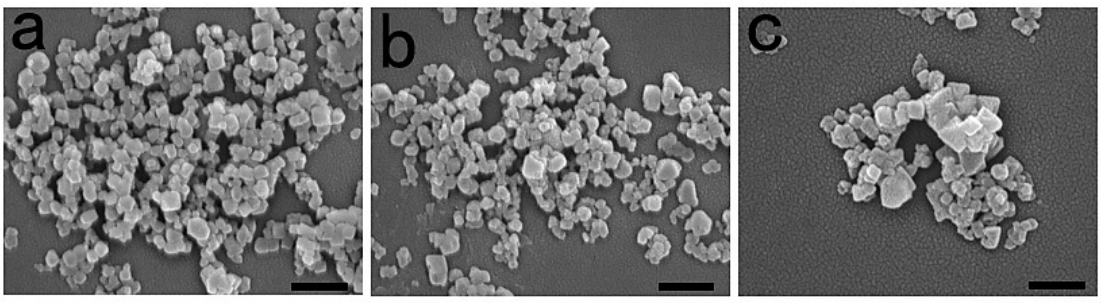

Fig. S1. SEM images of (a) UiO-66-COOH, (b) UiO-66-COOH-6 and (c) UiO-66-COOH-15. Scale bars were 500 nm.

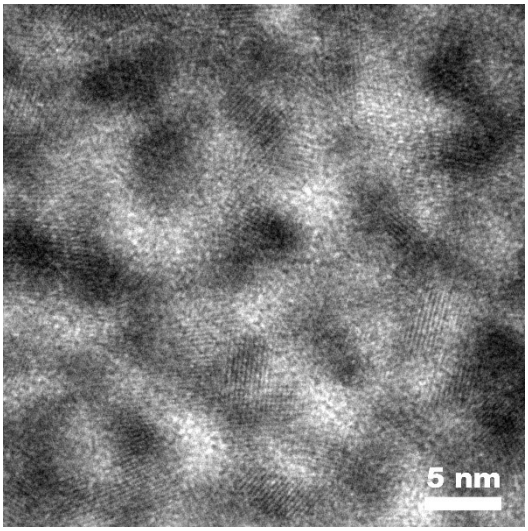

Fig. S2. HRTEM image of UiO-66-COOH-15.

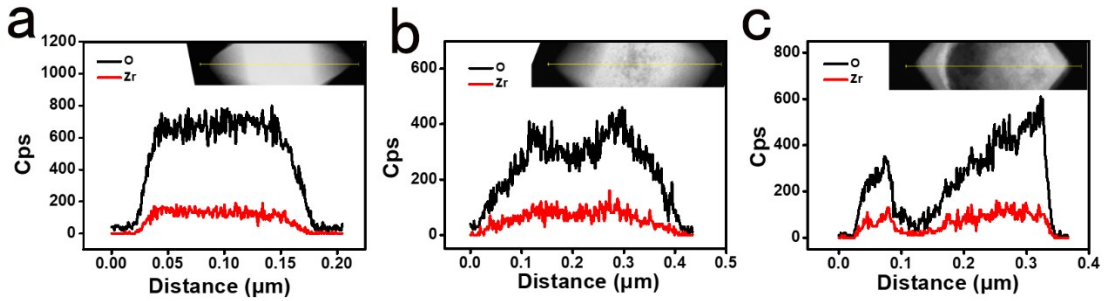

Fig. S3. Line scan pattern of (a) UiO-66-COOH, (b) UiO-66-COOH-6 and (c) UiO-66-COOH-15.

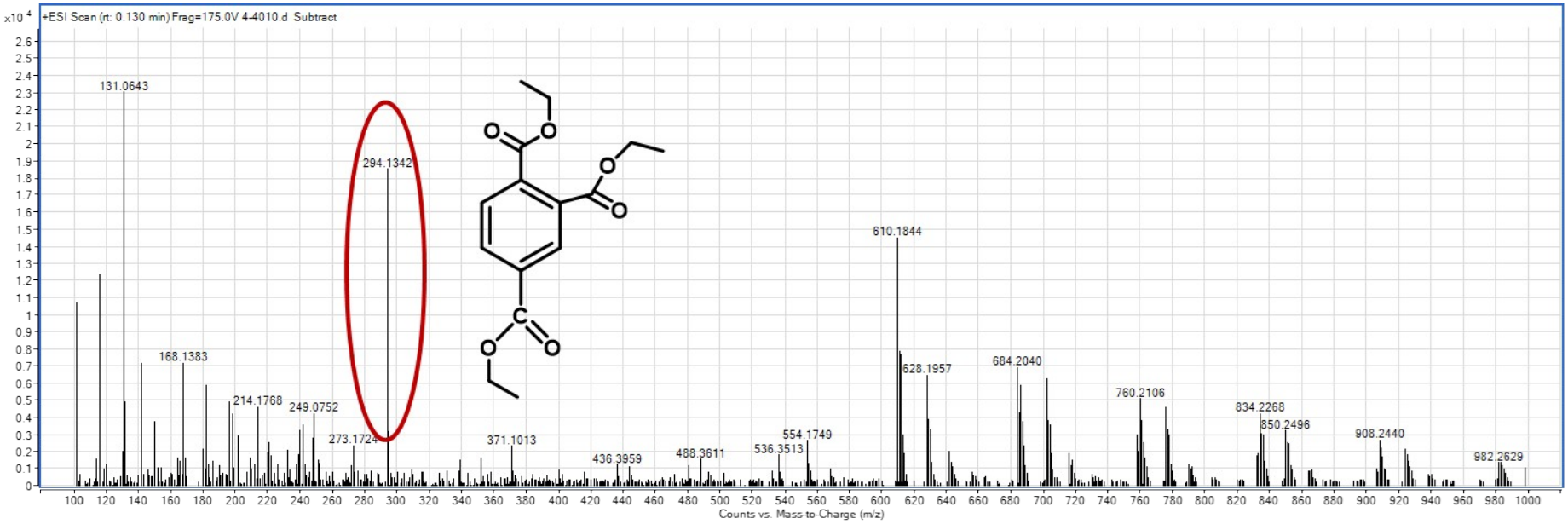

Fig. S4. Mass spectrum of the supernatant. m/z=294.1342 is consistent with the molecular weight of the ester formed by 1,2,4-benzenetricarboxylic acid and ethanol.

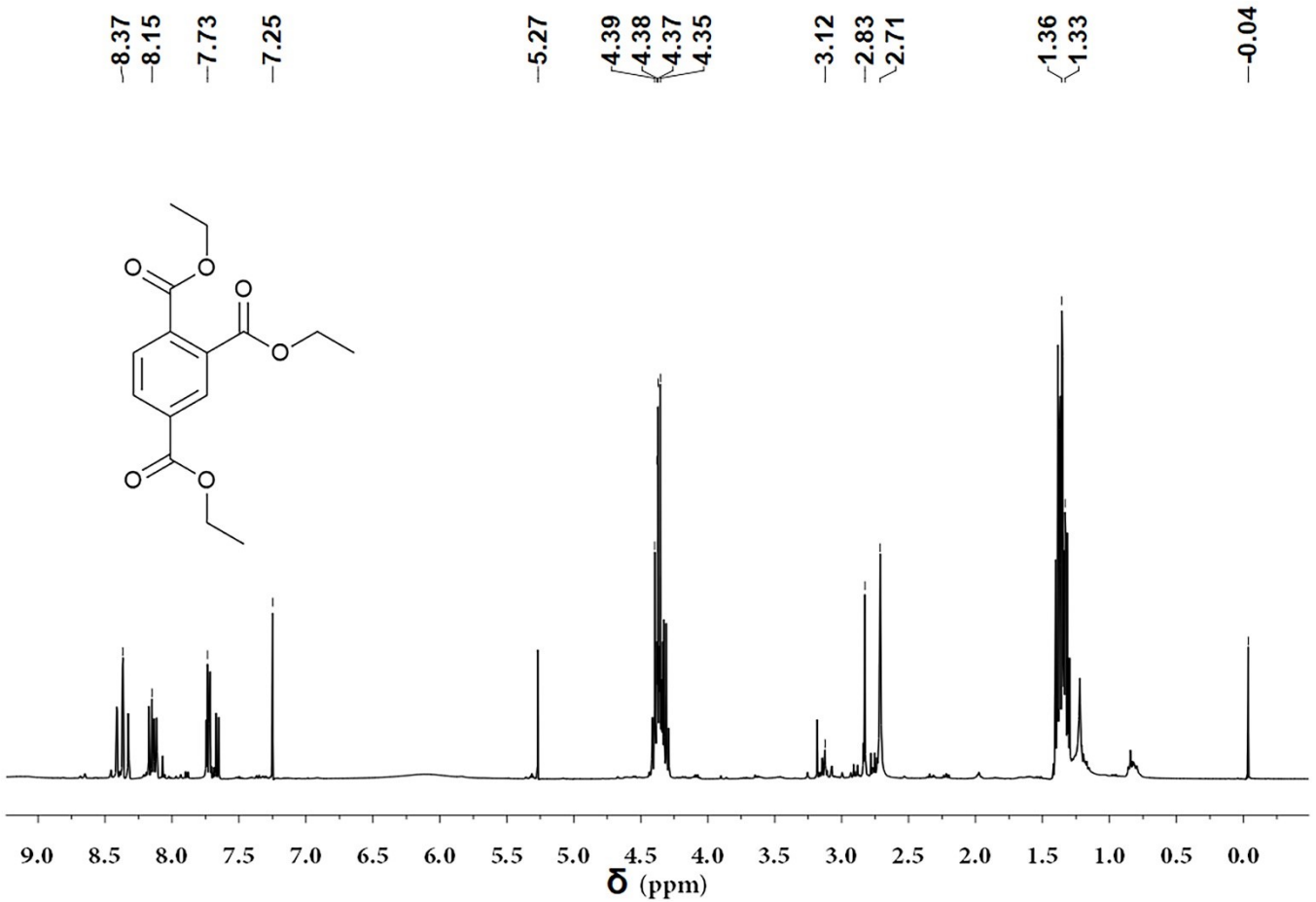

Fig. S5. ^{1}H NMR of the supernatant of UiO-66-COOH-12.

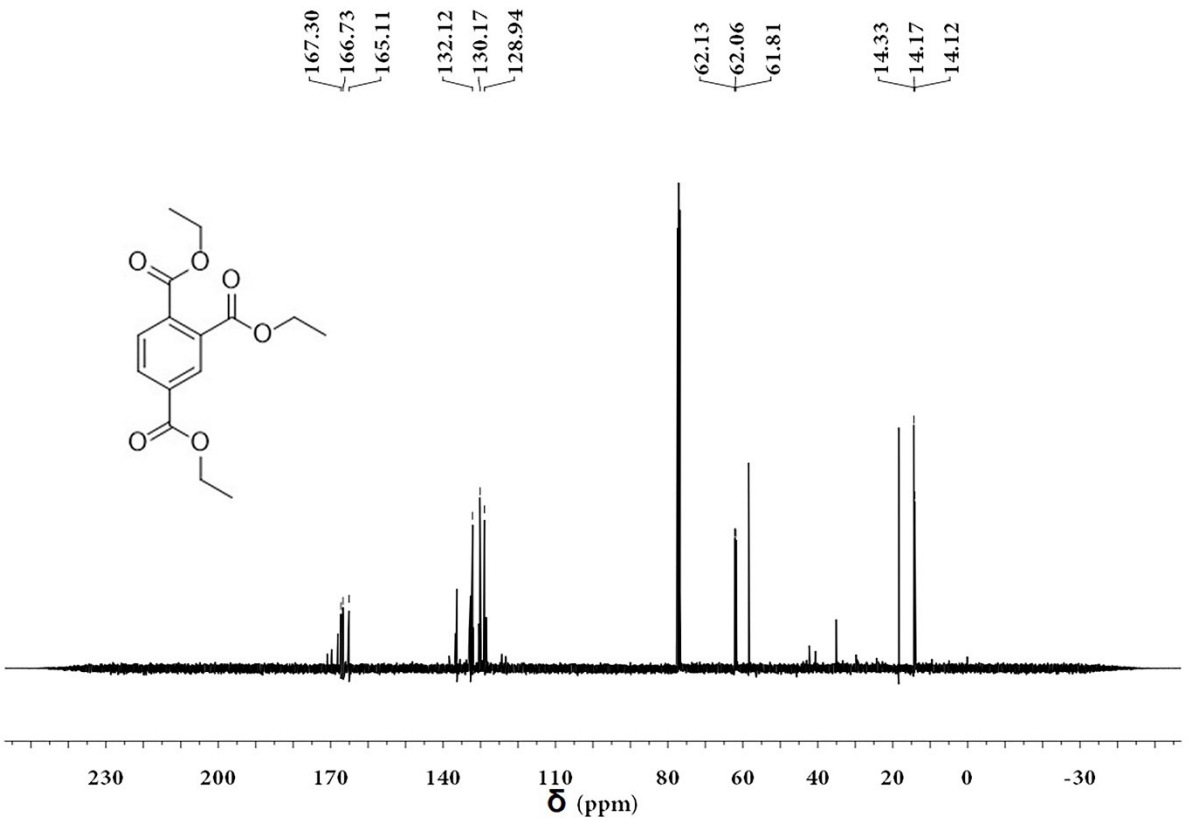

Fig. S6. ^{13}C NMR of the supernatant of UiO-66-COOH-12.

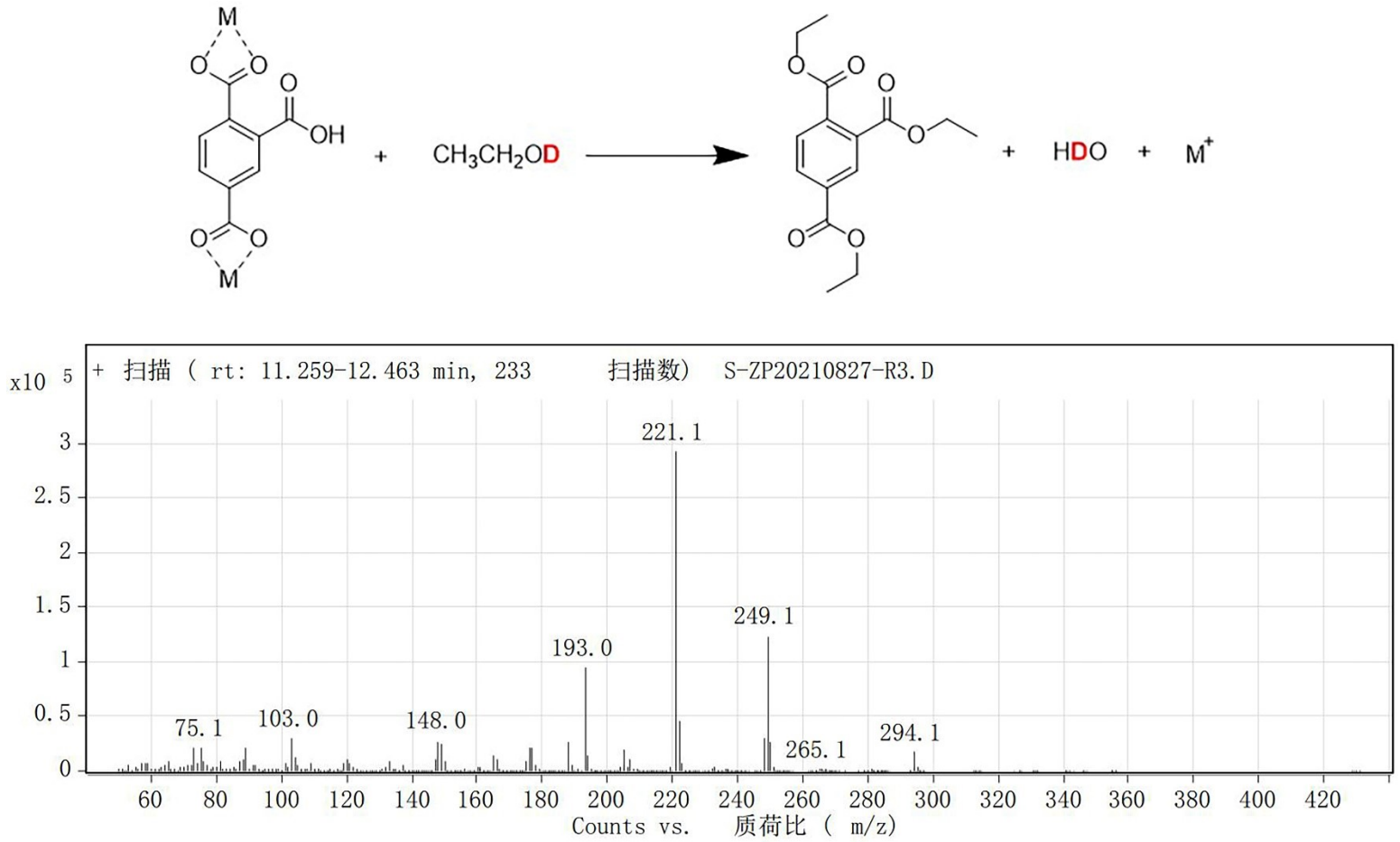

Fig. S7. MS of the supernatant of UiO-66-COOH treated with CH_3CH_2OD.

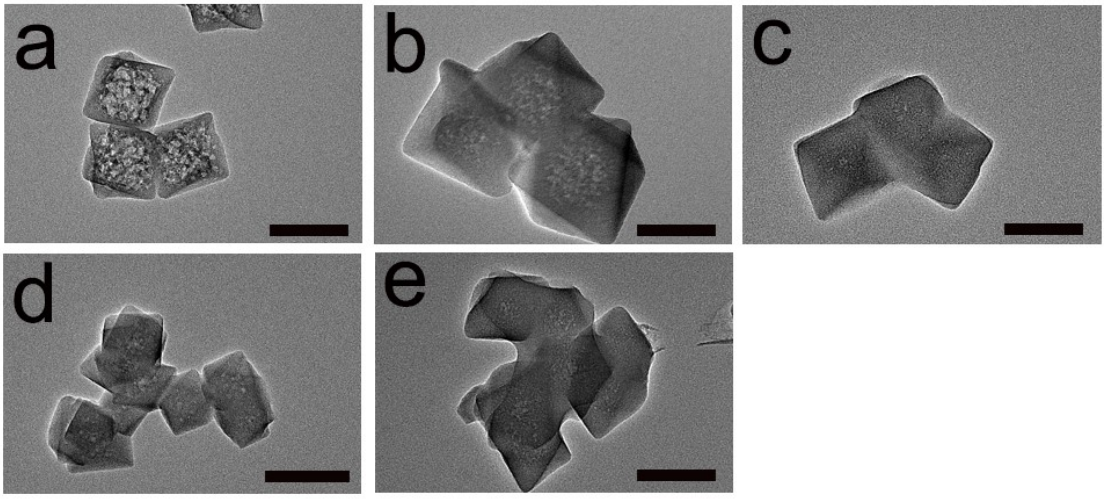

Fig. S8. TEM images of HP-UiO-66-COOH treated with different length of alcohols for different time. (a) methanol 3 h, (b) ethanol 9 h, (c) propanol 12 h, (d) butanol 24 h and (e) pentanol 36 h. Scale bars were 100 nm.

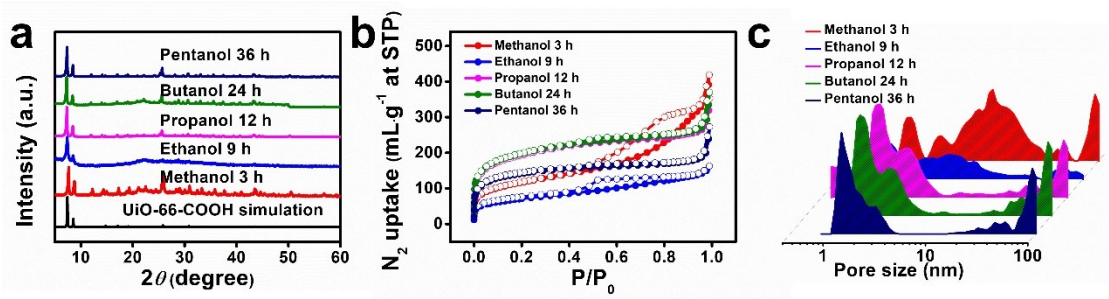

Fig. S9. (a) PXRD patterns of HP-UiO-66-COOH treated with different length of alcohols for different time. (b) N_2 adsorption–desorption isotherms of UiO-66-COOH treated with different length of alcohols for different time. (c) Pore-size distribution of UiO-66-COOH treated with different length of alcohols for different time.

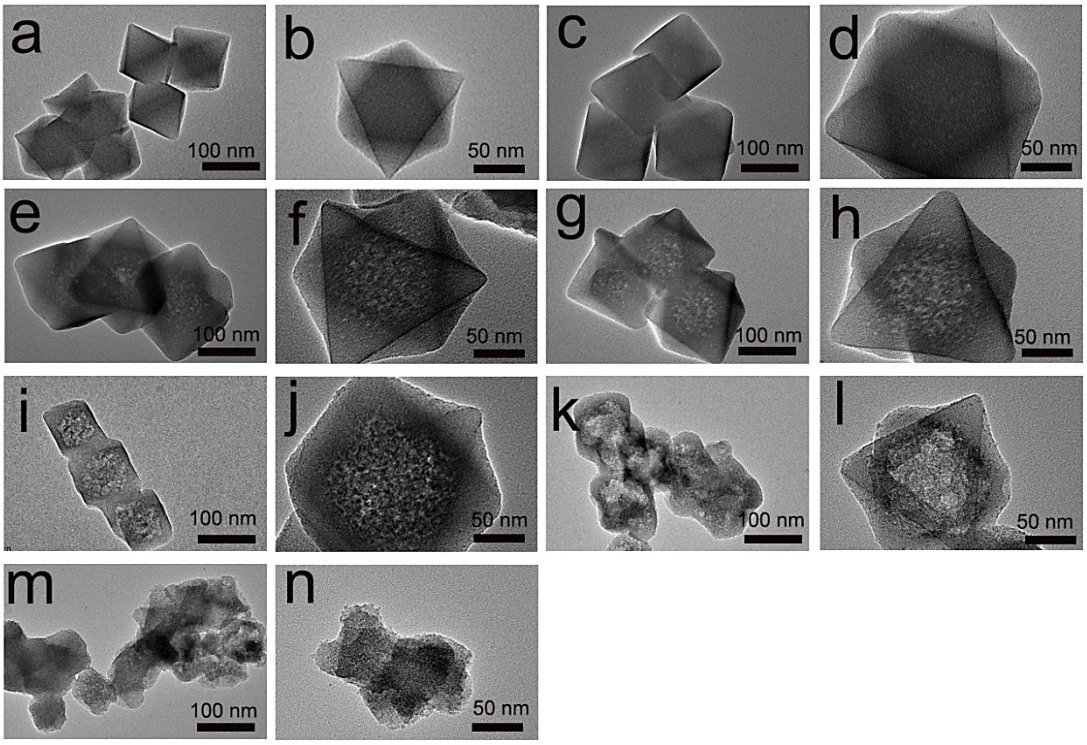

Fig. S10. TEM images of UiO-66-COOH treated by different time. (a,b) 0 h, (c,d) 3 h, (e,f) 6 h, (g,h) 9 h, (i,j) 12 h, (k,l) 15 h, (m,n) 24 h.

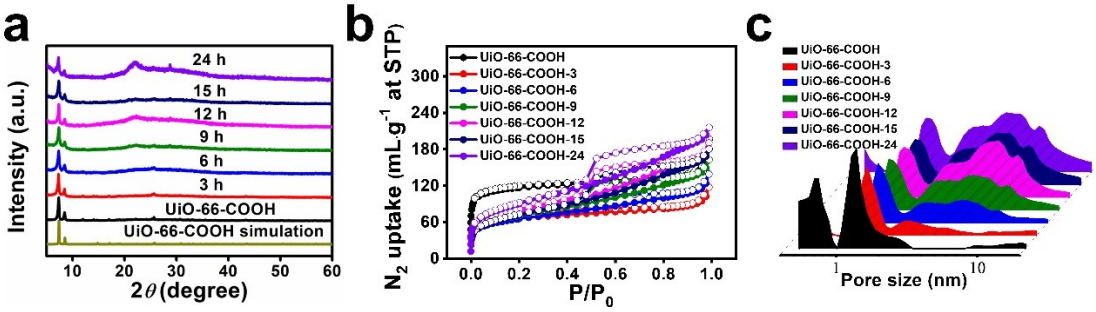

Fig. S11. (a) PXRD patterns of UiO-66-COOH treated by different time. (b) N_2 adsorption–desorption isotherms of UiO-66-COOH treated by different time. (c) Pore-size distribution of UiO-66-COOH treated with different time.

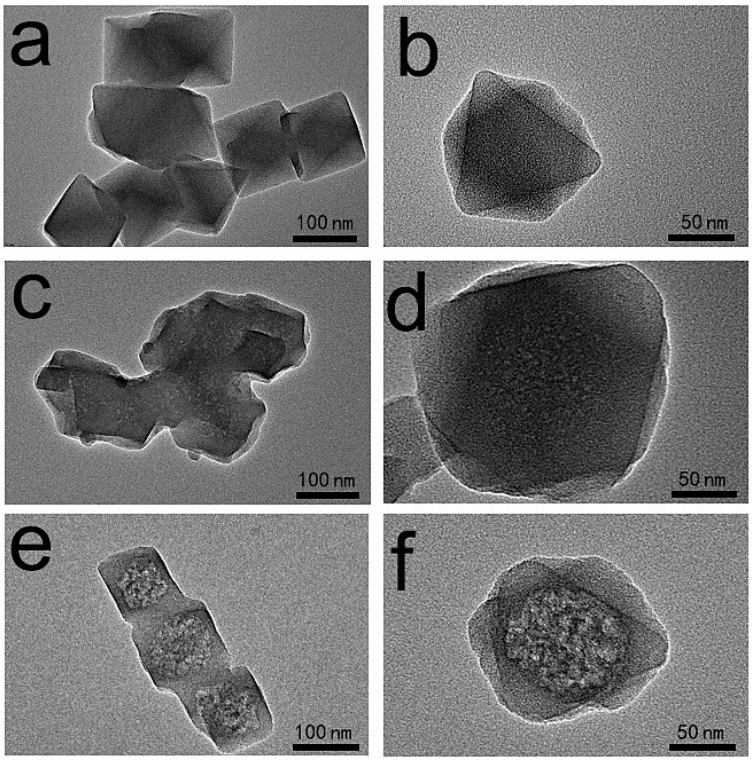

Fig. S12. TEM images of UiO-66-COOH treated with different temperature. (a,b) 60 °C, (c,d) 120 °C, (e,f) 180 °C.

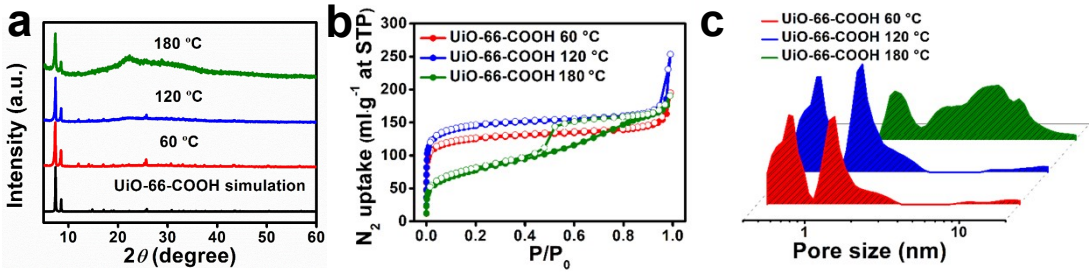

Fig. S13. (a) PXRD patterns of UiO-66-COOH treated by different temperature. (b) N_2 adsorption–desorption isotherms of UiO-66-COOH treated by different temperature. (c) pore-size distribution of UiO-66-COOH treated by different temperature.

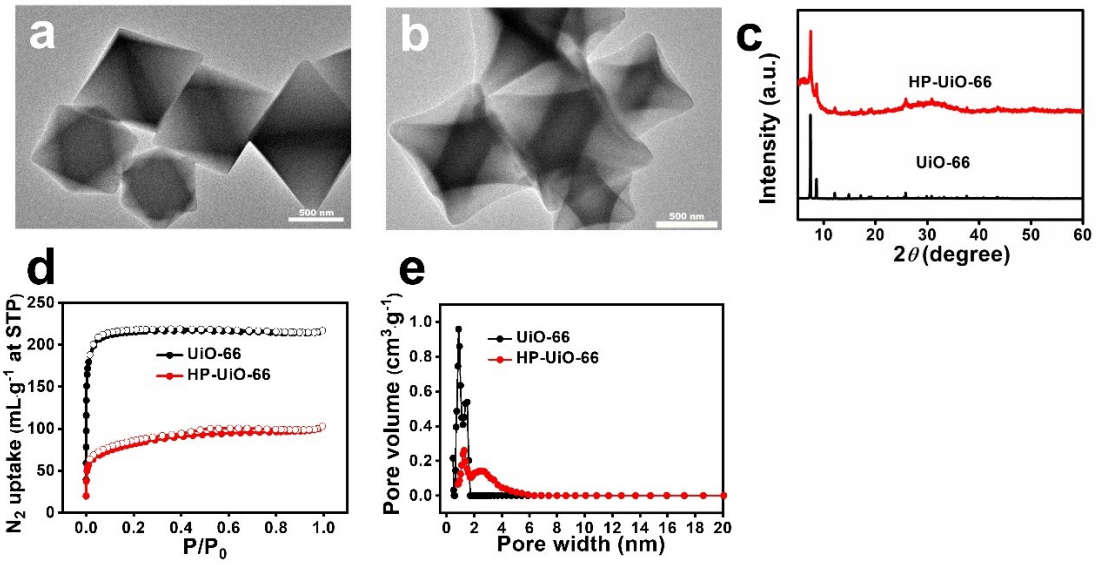

Fig. S14. TEM images of (a) UiO-66, (b) HP-UiO-66. (c) PXRD patterns of UiO-66 and HP-UiO-66. (d) N_2 adsorption–desorption isotherms of UiO-66 and HP-UiO-66. (e) Pore-size distribution of UiO-66 and HP-UiO-66.

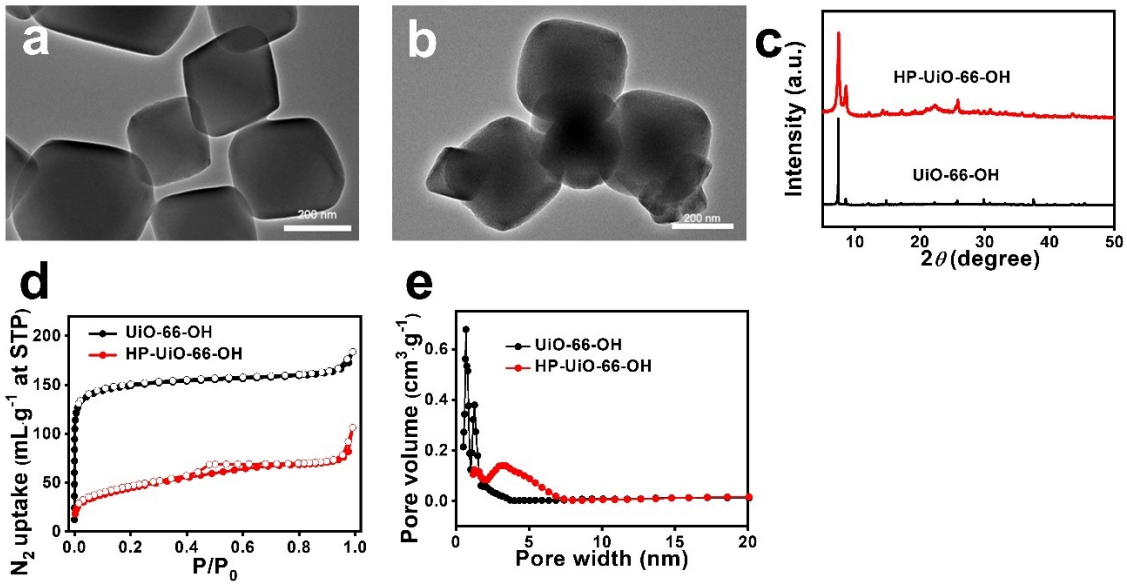

Fig. S15. TEM images of (a) UiO-66-OH, (b) HP-UiO-66-OH. (c) PXRD patterns of UiO-66-OH and HP-UiO-66-OH. (d) N_2 adsorption–desorption isotherms of UiO-66-OH and HP-UiO-66-OH. (e) Pore-size distribution of UiO-66-OH and HP-UiO-66-OH.

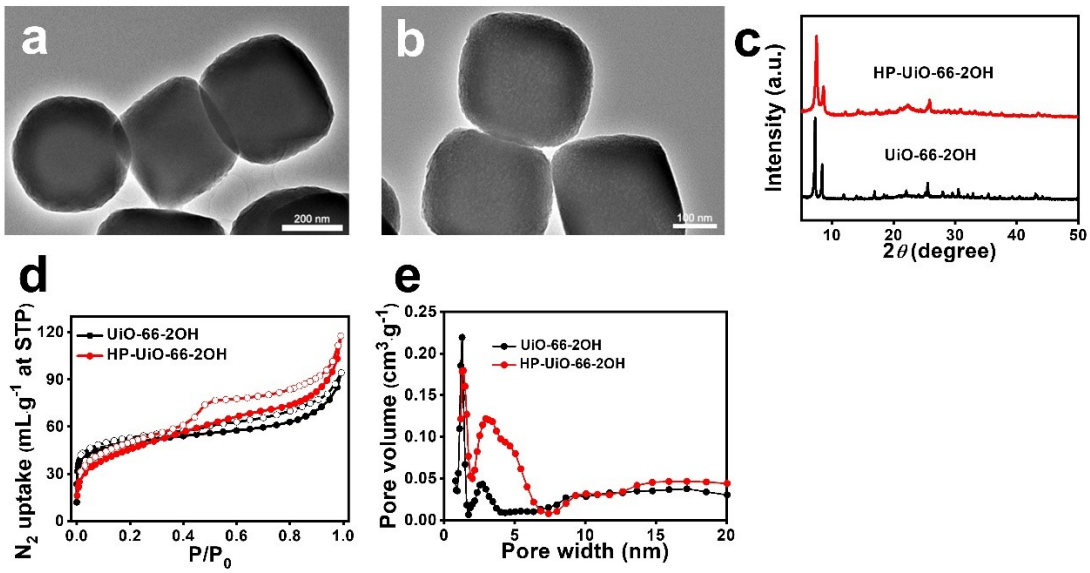

Fig. S16. TEM images of (a) UiO-66-2OH, (b) HP-UiO-66-2OH. (c) PXRD patterns of UiO-66-2OH and HP-UiO-66-2OH. (d) N_2 adsorption–desorption isotherms of UiO-66-2OH and HP-UiO-66-2OH. (e) Pore-size distribution of UiO-66-2OH and HP-UiO-66-2OH.

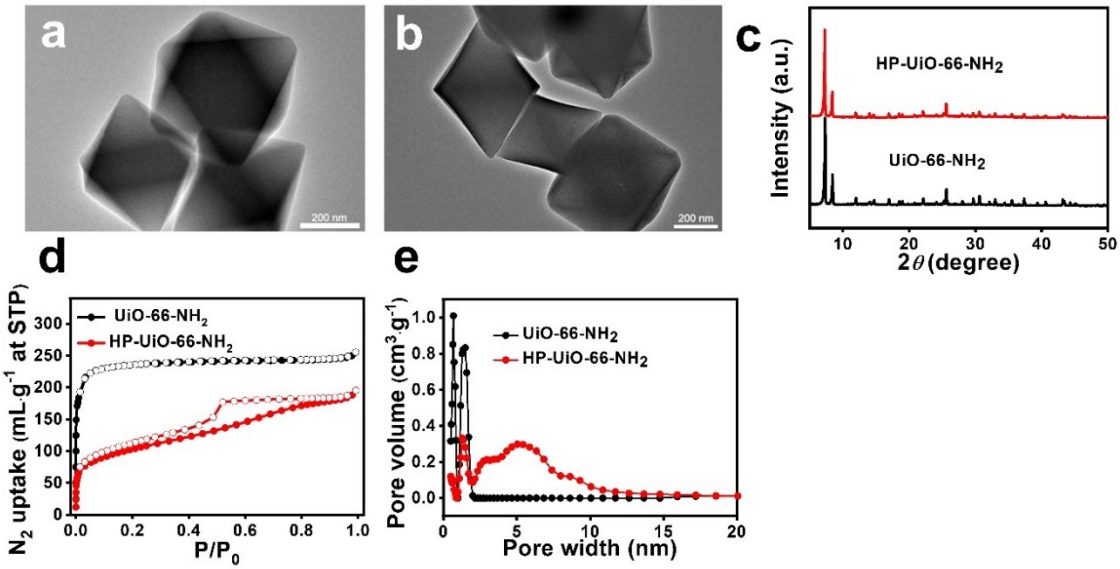

Fig. S17. TEM images of (a) UiO-66-NH_2, (b) HP-UiO-66-NH_2. (c) PXRD patterns of UiO-66-NH_2 and HP-UiO-66-NH_2. (d) N_2 adsorption–desorption isotherms of UiO-66-NH_2 and HP-UiO-66-NH_2. (e) Pore-size distribution of UiO-66-NH_2 and HP-UiO-66-NH_2.

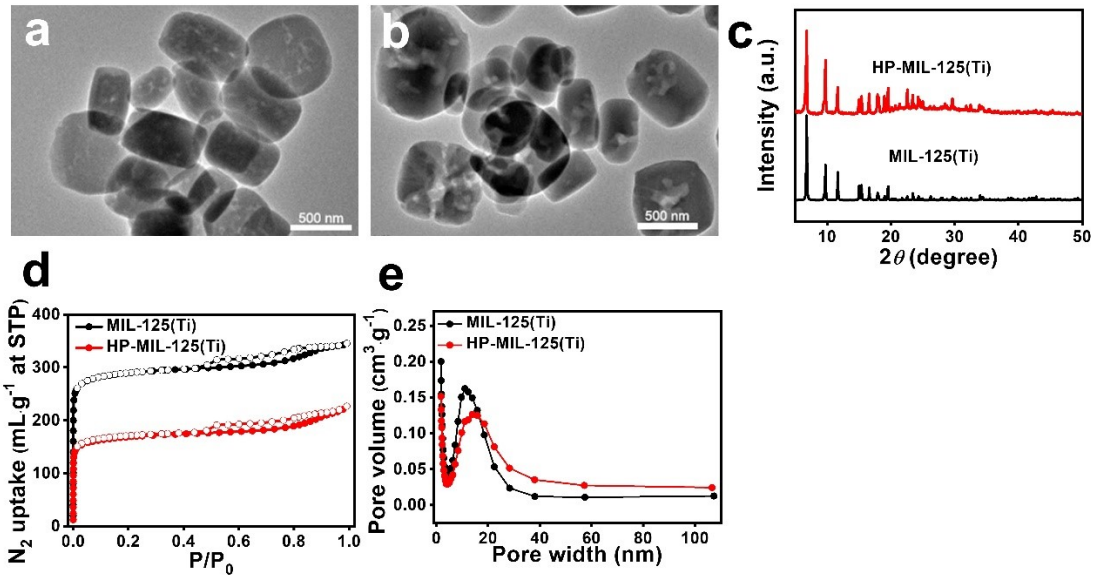

Fig. S18. TEM images of (a) MIL-125(Ti), (b) HP-MIL-125(Ti). (c) PXRD patterns of MIL-125(Ti) and HP-MIL-125(Ti). (d) N_2 adsorption–desorption isotherms of MIL-125(Ti) and HP-MIL-125(Ti). (e) Pore-size distribution of MIL-125(Ti) and HP-MIL-125(Ti).

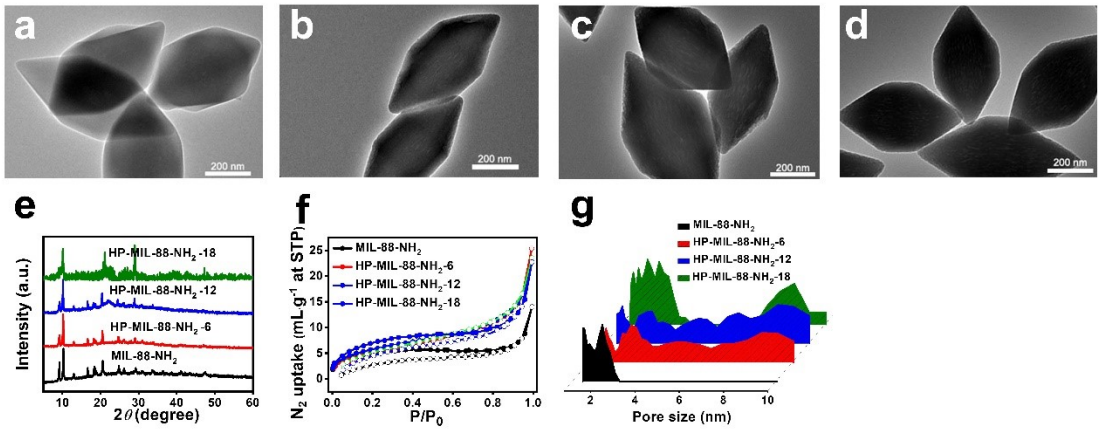

Fig. S19. TEM images of (a) MIL-88-NH_2, (b) HP-MIL-88-NH_2-6, (c) HP-MIL-88-NH_2-12, (d) HP-MIL-88-NH_2-18. (e) PXRD patterns of MIL-88-NH_2 and HP-MIL-88-NH_2. (f) N_2 adsorption–desorption isotherms of MIL-88-NH_2 and HP-MIL-88-NH_2. (g) Pore-size distribution of MIL-88-NH_2 and HP-MIL-88-NH_2.

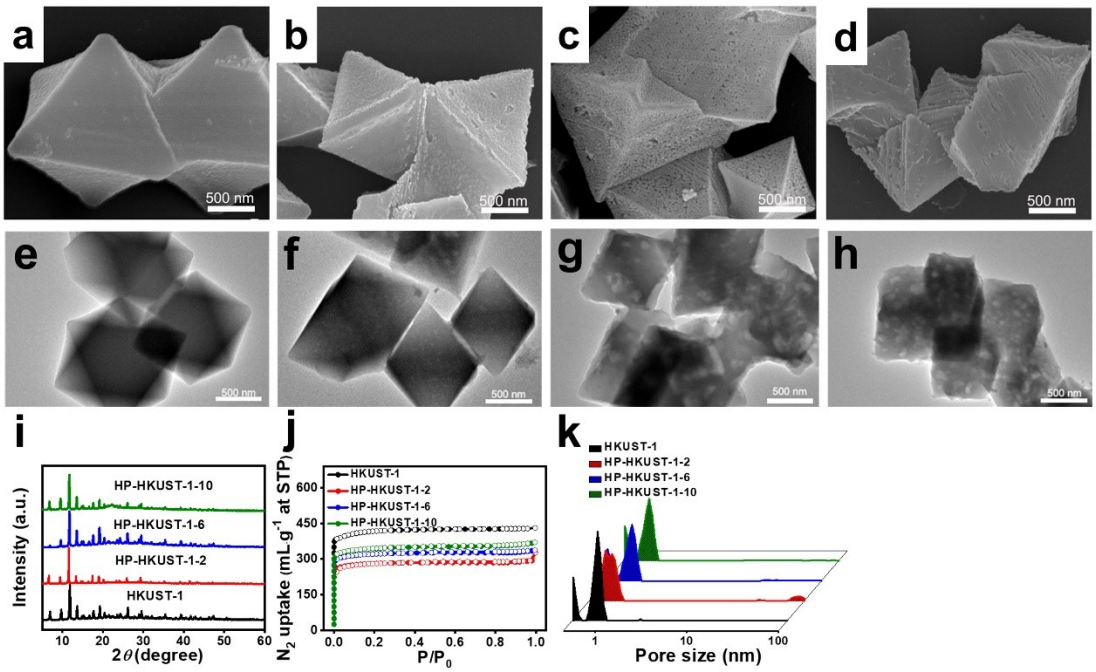

Fig. S20. TEM and SEM images of (a,e) HKUST-1, (b,f) HP-HKUST-1-2, (c,g) HP-HKUST-1-6, (d,h) HP-HKUST-1-10. (i) PXRD patterns of HKUST-1 and HP-HKUST-1. (j) N_2 adsorption–desorption isotherms of HKUST-1 and HP-HKUST-1. (k) Pore-size distribution of HKUST-1 and HP-HKUST-1.

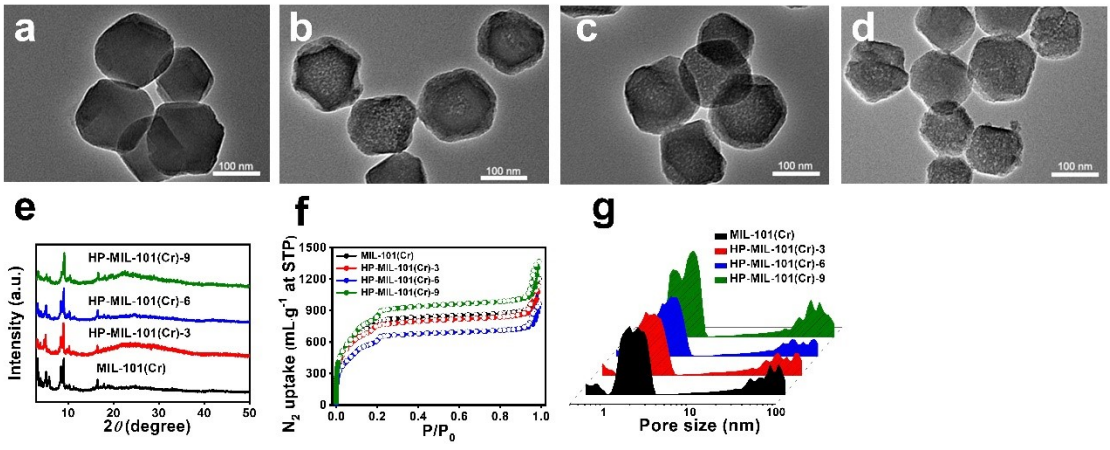

Fig. S21. TEM images of (a) MIL-101(Cr), (b) HP-MIL-101(Cr)-3, (c) HP-MIL-101(Cr)-6, (d) HP-MIL-101(Cr)-9. (e) PXRD patterns of MIL-101(Cr) and HP-MIL-101(Cr). (f) N_2 adsorption–desorption isotherms of MIL-101(Cr) and HP-MIL-101(Cr). (g) Pore-size distribution of MIL-101(Cr) and HP-MIL-101(Cr).

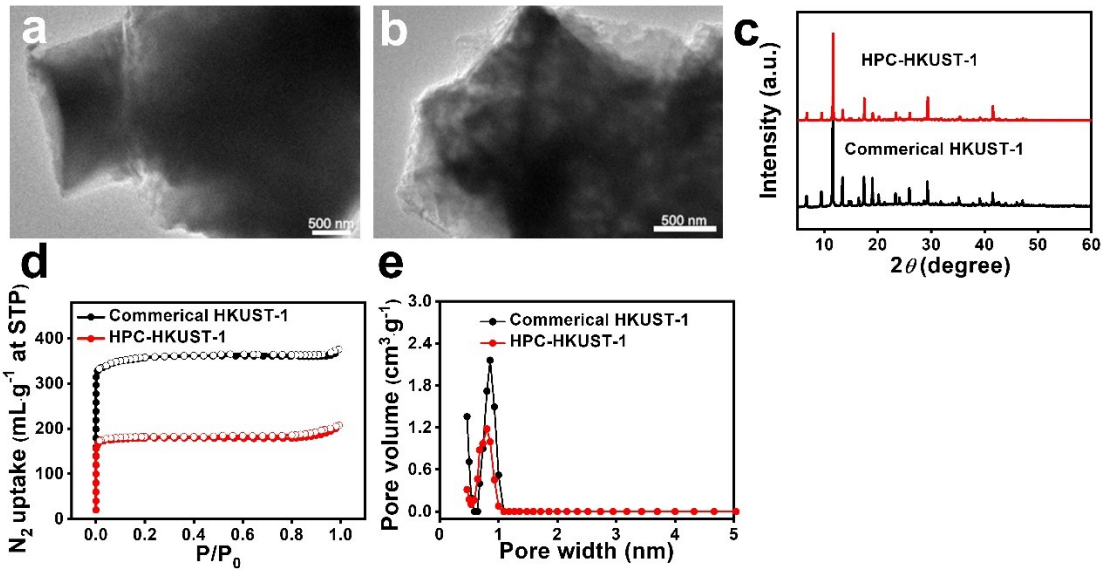

Fig. S22. TEM images of (a) commercial HKUST-1, (b) HPC-HKUST-1. (c) PXRD patterns of commercial HKUST-1 and HPC-HKUST-1. (d) N_2 adsorption–desorption isotherms of commercial HKUST-1 and HPC-HKUST-1. (e) Pore-size distribution of commercial HKUST-1 and HPC-HKUST-1.

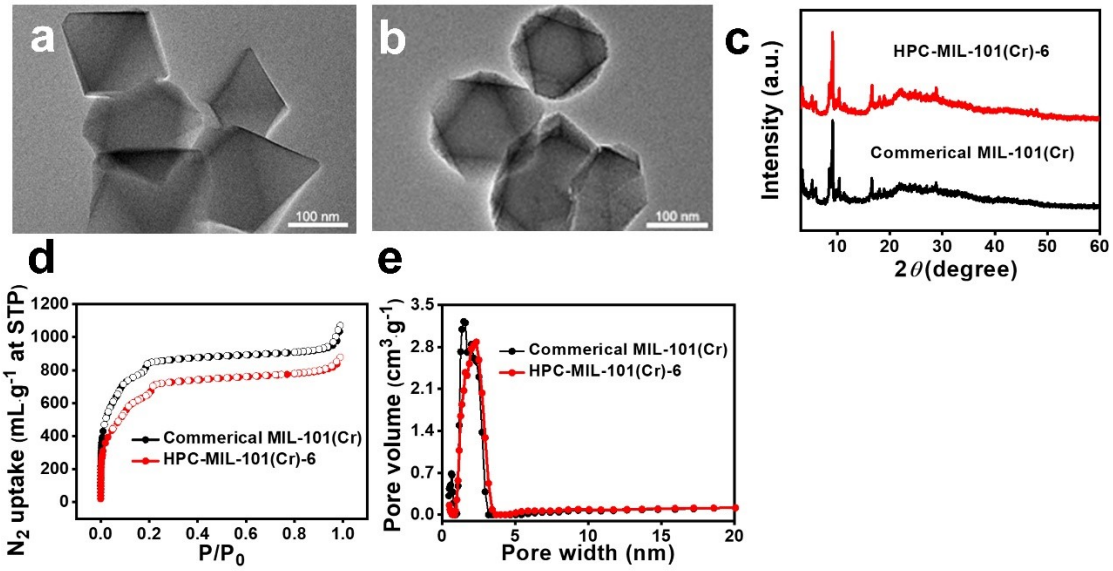

Fig. S23. TEM images of (a) commercial MIL-101(Cr), (b) HPC-MIL-101(Cr). (c) PXRD patterns of commercial MIL-101(Cr) and HPC-MIL-101(Cr). (d) N_2 adsorption–desorption isotherms of commercial MIL-101(Cr) and HPC-MIL-101(Cr). (e) Pore-size distribution of commercial MIL-101(Cr) and HPC-MIL-101(Cr).

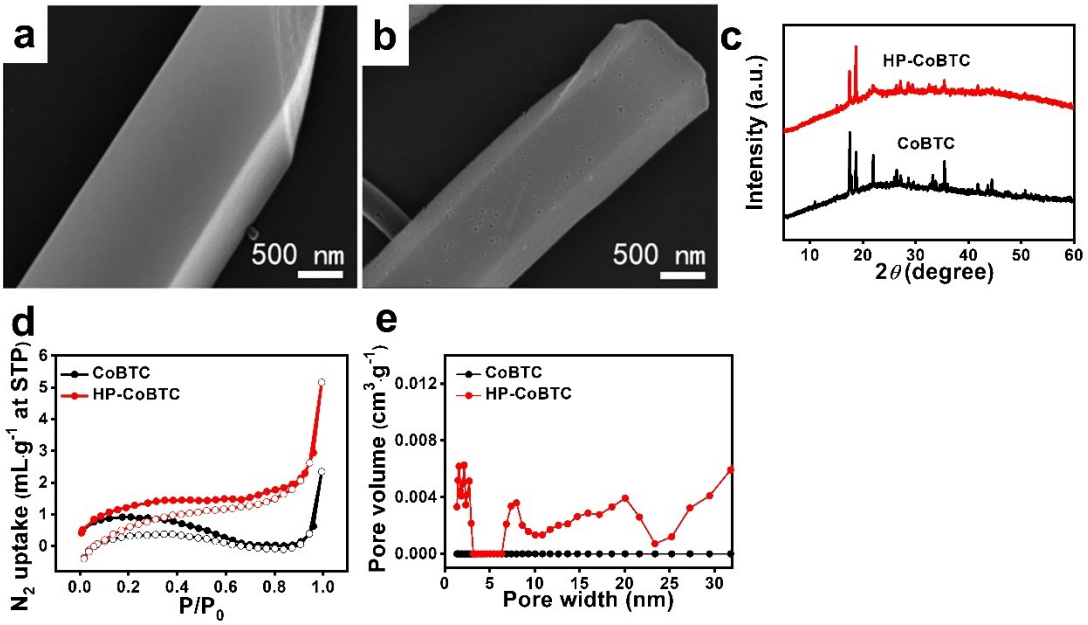

Fig. S24. SEM images of (a) CoBTC, (b) HP-CoBTC. (c) PXRD patterns of CoBTC and HP-CoBTC. (d) N_2 adsorption–desorption isotherms of CoBTC and HP-CoBTC. (e) Pore-size distribution of commercial CoBTC and HP-CoBTC.

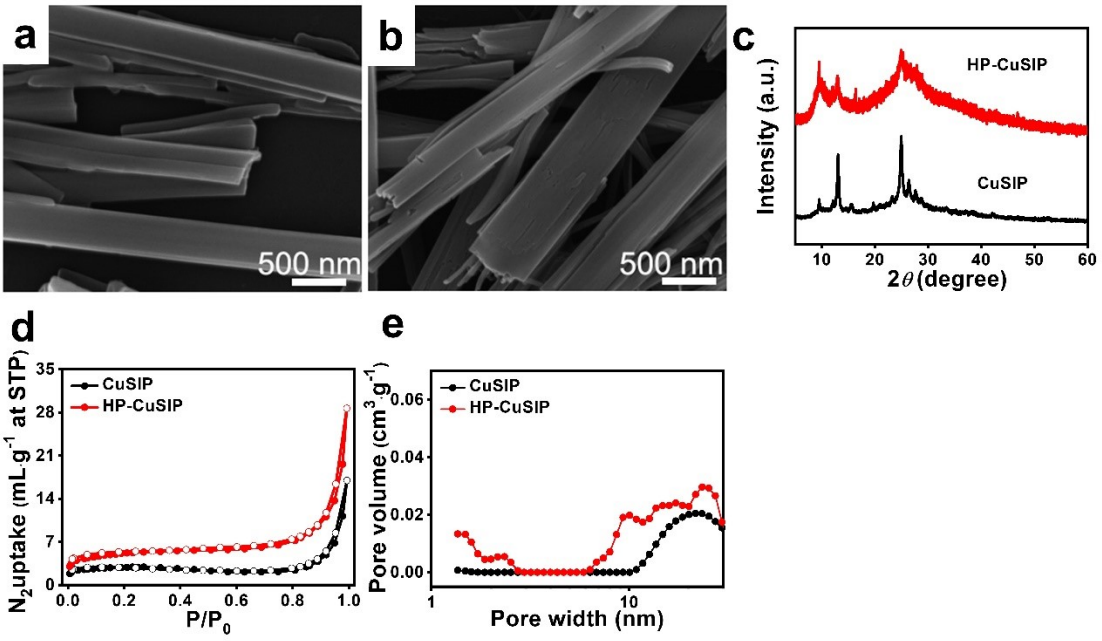

Fig. S25. SEM images of (a) CuSIP, (b) HP-CuSIP. (c) PXRD patterns of CuSIP and HP-CuSIP. (d) N_2 adsorption–desorption isotherms of CuSIP and HP-CuSIP. (e) Pore-size distribution of CuSIP and HP-CuSIP.

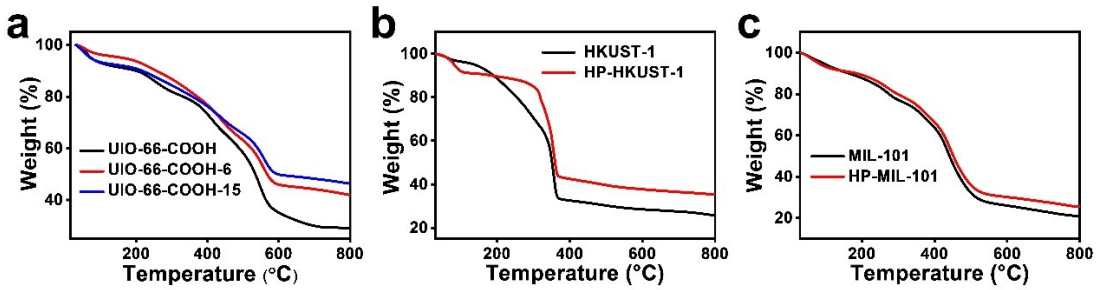

Fig. S26. TGA spectra of (a) UiO-66-COOH, UiO-66-COOH-6 and UiO-66-COOH-15. (b) HKUST-1 and HP-HKUST-1. (c) MIL-101 and HP-MIL-101.

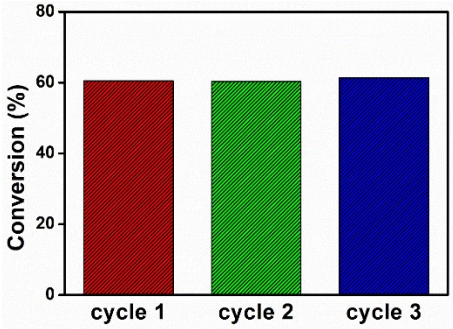

Fig. S27. The reusability of UiO-66-COOH-15 composites in the ring-opening reaction of styrene oxide for three consecutive runs.

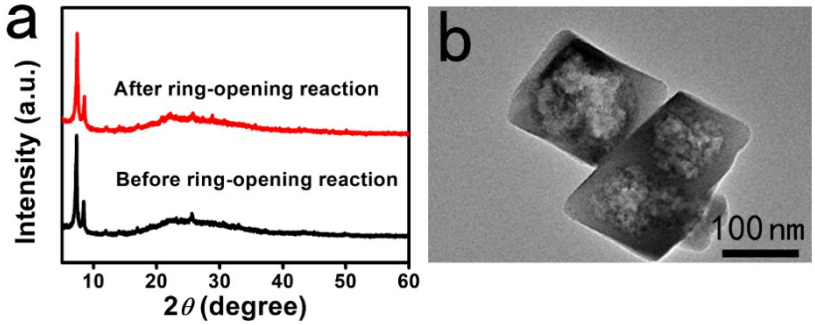

Fig. S28. Ring-opening reaction of styrene oxide by UiO-66-COOH-15 composites. (a) PXRD patterns of UiO-66-COOH-15 composites before and after ring-opening of styrene oxide reaction for three consecutive runs. (b) TEM image of UiO-66-COOH-15 composites after ring-opening reaction of styrene oxide.

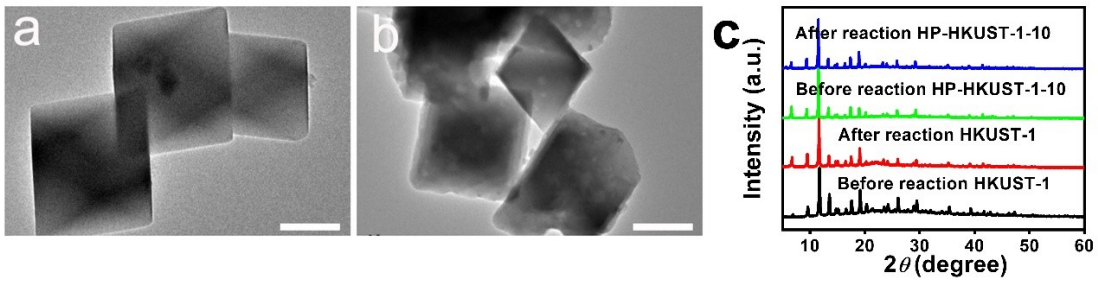

Fig. S29. TEM image of HKUST-1 and HP-HKUST-1 composites after oxidation of diphenylmethane. (a) HKUST-1, (b) HP-HKUST-1. Scale bars were 500 nm. (c) PXRD patterns of HKUST-1 and HP-HKUST-1 composites before and after oxidation of diphenylmethane.

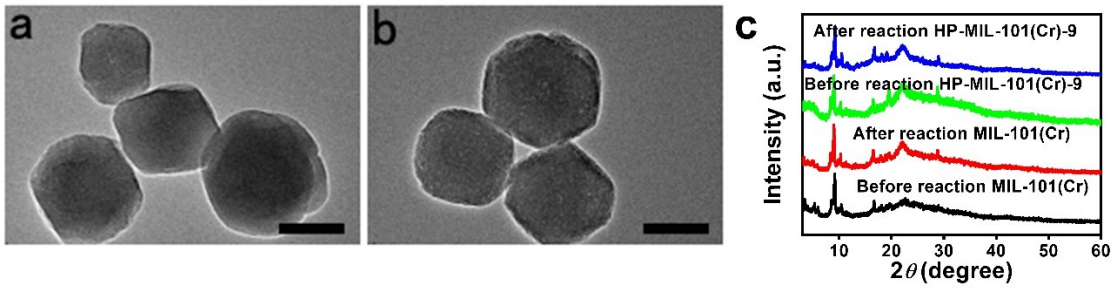

Fig. S30. TEM image of MIL-101(Cr) and HP-MIL-101(Cr) composites after oxidation of styrene. (a) MIL-101(Cr), (b) HP-MIL-101(Cr). Scale bars were 100 nm. (c) PXRD patterns of MIL-101(Cr) and HP-MIL-101(Cr) composites before and after oxidation of styrene

Table S1: Porosity analysis of UiO-66-COOH and other MOFs and CPs treated under different conditions.

MOFs/CP	Solvent	Temperature (°C)	Time (h)	S_{BET}[a] (m^2g^{-1})	V_t[b] (cm^3g^{-1})	V_{meso}[c] (cm^3g^{-1})	V_{meso}/V_{micro}	D_{micro}[d] (nm)	D_{meso}[d] (nm)
UiO-66-COOH	--	--	--	444.09	0.30	0.15	0.98	0.68,1.27	--
HP-UiO-66-COOH	Methanol	180	3	411.10	0.65	0.60	12.00	1.48	2.94-54.42
HP-UiO-66-COOH-9	Ethanol	180	9	244.48	0.25	0.21	5.25	1.36	3.34-20
HP-UiO-66-COOH	Propanol	180	12	693.70	0.55	0.36	1.89	0.68,1.48	2.73-20
HP-UiO-66-COOH	Butanol	180	24	714.62	0.57	0.38	2.00	1.36	2.73-20
HP-UiO-66-COOH	Pentanol	180	36	524.51	0.42	0.27	1.80	1.36	2.73-20
HP-UiO-66-COOH	Ethanol	60	12	464.79	0.30	0.14	0.87	0.64,1.27	--
HP-UiO-66-COOH	Ethanol	120	12	530.73	0.39	0.20	1.05	0.68,1.27	9.31
HP-UiO-66-COOH-12	Ethanol	180	12	270.22	0.30	0.25	5.00	1.36	3.43-20

HP-UiO-66-COOH-3	Ethanol	180	3	241.51	0.18	0.11	1.57	1.27	2.95-20
HP-UiO-66-COOH-6	Ethanol	180	6	233.20	0.22	0.16	2.67	1.27	3.34-20
HP-UiO-66-COOH-15	Ethanol	180	15	248.97	0.28	0.24	6.00	1.36	3.34-20
HP-UiO-66-COOH-24	Ethanol	180	24	312.66	0.33	0.29	7.25	1.09,1.36	3.34-20
UiO-66	--	--	--	676.67	0.335	0.015	0.05	0.86,1.48	--
HP-UiO-66-7	Ethanol	180	7	298.59	0.159	0.072	0.82	1.27	2.52
UiO-66-OH	Ethanol	--	--	557.44	0.28	0.08	0.40	0.68,1.27	--
HP-UiO-66-OH-12	Ethanol	180	12	162.28	0.16	0.14	7.00	1.27	3.18
UiO-66-2OH	--	--	--	179.36	0.15	0.09	1.5	1.27	2.73-20
HP-UiO-66-2OH-12	Ethanol	180	12	149.64	0.18	0.17	17	1.37	2.95-20
UiO-66-NH_2	--	--	--	934.54	0.40	0.05	0.14	0.68,1.48	--
HP-UiO-66-NH_2-24	Ethanol	180	24	337.99	0.30	0.23	3.28	0.64,1.27	2.95,5.04
MIL-125(Ti)	--	--	--	1107.24	0.53	0.13	0.32	--	11.08

HP-MIL-125(Ti)-0.5	Ethanol	180	0.5	585.71	0.41	0.12	0.41	--	13.89
MIL-88-NH_2	--	--	--	17.55	0.022	0.018	4.50	--	2.09,2.65
HP-MIL-88-NH_2-6	Ethanol	120	6	20.17	0.039	0.037	18.50	--	2.19-5.55
HP-MIL-88-NH_2-12	Ethanol	120	12	20.91	0.036	0.035	35.00	--	2.52-10
HP-MIL-88-NH_2-18	Ethanol	120	18	25.36	0.035	0.032	10.67	--	2.00-10
HKUST-1	--	--	--	1654.11	0.667	0.058	0.09	0.86	--
HP-HKUST-1-2	Ethanol	180	2	1126.58	0.506	0.039	0.08	0.68,0.80	--
HP-HKUST-1-6	Ethanol	180	6	1284.97	0.521	0.050	0.11	0.86	--
HP-HKUST-1-10	Ethanol	180	10	1374.08	0.573	0.073	0.15	0.86	--
MIL-101(Cr)	--	--	--	3015.06	1.861	1.111	1.54	0.64,1.60	9.3
HP-MIL-101(Cr)-3	Ethanol	180	3	2739.58	1.754	1.177	2.03	1.6	2-50
HP-MIL-101(Cr)-6	Ethanol	180	6	2364.98	1.490	0.939	1.70	--	2-50
HP-MIL-101(Cr)-9	Ethanol	180	9	3280.13	2.116	1.380	1.88	0.59,1.36	2-50

CoBTC	--	--	--	2.77	--	--	--	--	--
HP-CoBTC-2	Ethanol	80	2	4.51	0.008	0.007	7.00	1.59	2.16,2.73
CuSIP	--	--	--	--	--	--	--	--	--
HP-CuSIP-3	Ethanol	80	3	18.30	0.057	0.051	8.50	--	2.34,10.06
C-HKUST-1	--	--	--	1461.57	0.581	0.091	0.186	0.68,0.86	--
HPC-HKUST-1-10	Ethanol	180	10	684.86	0.321	0.057	0.215	0.80	15.94
C-MIL-101	--	--	--	2905.67	1.657	0.814	0.966	0.64,1.48	9.31
HPC-MIL-101-6	Ethanol	180	6	2360.81	1.359	0.705	1.078	--	2.34,4.6-20

References

1. X. Zhao, D. Liu, H. Huang and C. Zhong, *Micropor. Mesopor. Mat.,* 2016, **224**, 149-154.
2. W. Zhang, B. Zheng, W. Shi, X. Chen, Z. Xu, S. Li, Y. R. Chi, Y. Yang, J. Lu, W. Huang and F. Huo, *Adv. Mater.*, 2018, **30**, 1800643.
3. Y. Fu, D. Sun, Y. Chen, R. Huang, Z. Ding, X. Fu and Z. Li, *Angew. Chem., Int. Ed.,* 2012, **51**, 3364-3367.
4. J. F. Kurisingal, Y. Rachuri, Y. Gu, Y. Choe and D.-W. Park, *Inorg. Chem. Front.,* 2019, **6**, 3613-3620.

5. J.-L. Zhuang, D. Ceglarek, S. Pethuraj and A. Terfort, *Adv. Funct. Mater.,* 2011, **21**, 1442-1447.

6. W. Liu, J. Huang, Q. Yang, S. Wang, X. Sun, W. Zhang, J. Liu and F. Huo, *Angew. Chem., Int. Ed.* 2017, **56**, 5512-5516.

7. C. Li, X. Lou, M. Shen, X. Hu, Z. Guo, Y. Wang, B. Hu and Q. Chen, *ACS Appl. Mater. Interfaces.*, 2016, **8**, 15352-15360.

8. B. Xiao, P. J. Byrne, P. S. Wheatley, D. S. Wragg, X. Zhao, A. J. Fletcher, K. M. Thomas, L. Peters, J. S. Evans, J. E. Warren, W. Zhou and R. E. Morris, *Nat. Chem.*, 2009, **1**, 289-294.

9. A. Dhakshinamoorthy, M. Alvaro and H. Garcia, *Chem. Eng. J.,* 2010, **16**, 8530-8536.

10. D. Kishore and A. E. Rodrigues, *Catal. Commun.,* 2009, **10**, 1212-1215.